Dermal Uptake of Organic Vapors Commonly Found in Indoor Air

Charles J. Weschler[1,2*] and William W Nazaroff[3]

[1]Environmental and Occupational Health Sciences Institute, Rutgers University, Piscataway, NJ 08854, USA
[2]International Centre for Indoor Environment and Energy, Technical University of Denmark, DK-2800 Lyngby, Denmark
[3]Department of Civil and Environmental Engineering, University of California, Berkeley, CA 94720-1710 USA

Supporting Information

32   **S1. Calculating transdermal permeability coefficients.** To calculate k_{p_g} for a given

33   organic compound, we begin by using SPARC v4.6

34   (http://archemcalc.com/sparc/test/login.cfm?CFID=14923&CFTOKEN=18639285) to calculate

35   the values at 32 °C of the compound's octanol-water partition coefficient, K_{ow} (dimensionless)

36   and Henry's constant, H (in units of (moles per liter) per atmosphere). We then use a

37   deterministic model proposed by Mitragotri [1] to calculate the compound's permeability

38   coefficient through the stratum corneum when the vehicle in contact with the skin is water

39   (k_{p_cw}):

40         $\log (k_{p\_cw}) = 0.7 \log (K_{ow}) - 0.0722(MW^{2/3}) - 5.252$ (S1)

41   Here, MW is the compound's molecular weight (g/mol) and k_{p_cw} is in units of cm s^{-1}. A

42   relationship developed by Bunge et al. [2] is used to estimate B, the ratio of a compound's

43   stratum corneum permeability coefficient (k_{p_cw}) to its viable epidermis permeability coefficient

44   (k_{p_ew}):

45         $B = [k_{p\_cw} \times (MW)^{0.5}]/(2.6 \text{ cm h}^{-1})$ (S2)

46   where k_{p_cw} is expressed in units of cm h^{-1}. The value of B is then used to estimate the

47   compound's permeability coefficient through the stratum corneum/viable epidermis composite

48   when the vehicle in contact with the skin is water (k_{p_w}):

49         $k_{p\_w} = k_{p\_cw}/(1 + B)$ (S3)

50   The permeability coefficient through the stratum corneum/viable epidermis composite when

51   the vehicle in contact with the skin is air (k_{p_b}) is calculated using Henry's constant:

52         $k_{p\_b} = k_{p\_w} \times (HRT)$ (S4)

53   where R is the gas constant (0.0821 atm liter mole^{-1} K^{-1}) and T is the skin temperature (305 K =

54   32 °C). Finally the overall "indoor air transdermal permeability coefficient," k_{p_g}, is calculated

55   using a resistor-in-series model:

56        $1/k_{p\_g} = 1/v_d + 1/k_{p\_b}$ (S5)

57   Here, v_d is the mass-transfer coefficient that describes the external transport of a compound from

58   the gas phase in the core of a room through the boundary layer adjacent to the skin. Throughout

59   the work reported in this paper, we assume that $v_d \sim 6$ m h^{-1} [3].

60   **S2. Calculating maximum flux for DEP and DnBP vapors.** For air saturated with vapors,

61   we calculate a maximum flux for direct dermal absorption of 4600 µg m^{-2} h^{-1} for DEP and 185

62   µg m^{-2} h^{-1} for DnBP. These fluxes are calculated as the product of the gas phase concentration

63   (C_g) and the overall permeability coefficient (k_{p_g}) – see equation (3) in the main text. The

64   saturated gas-phase concentrations of DEP and DnBP are calculated from their respective vapor

65   pressures (P_s) at 25 °C. For DEP, $P_s = 1.5 \times 10^{-7}$ atm and for DnBP, $P_s = 3.4 \times 10^{-9}$ atm (values

66   calculated using SPARC v4.6). These vapor pressures are equivalent to gas-phase concentrations

67   of 1360 µg m^{-3} for DEP and 39 µg m^{-3} for DnBP. The values for k_{p_g} are taken from Table S1 –

68   3.4 m/h for DEP and 4.8 m/h for DnBP. Hence, the flux for DEP is 1360 µg/m^3 × 3.4 m/h = 4600

69   µg m^{-2} h^{-1}, while the flux for DnBP is 39 µg/m^3× 4.8 m/h = 185 µg m^{-2} h^{-1}.

70   **S3. Time scale to achieve steady state.** The values for k_{p_g} listed in Table S1 apply for

71   steady-state conditions. The time required for a steady-state model to serve as a reasonable

72   representation of the transdermal permeation process can be approximated by the time scale

73   necessary for an organic compound to achieve equilibrium sorption with skin-surface lipids by

74   means of transport from the gas-phase, τ_s [3]. Under typical living conditions, there may be

75 insufficient time for this to occur for some compounds. We have previously written that τ_s can be

76 estimated as

77 $\qquad \tau_s \sim K_{\text{lg}}\, X/v_{\text{d}}$ (S6)

78 where K_{lg} is the equilibrium partitioning coefficient between skin-surface lipids and the gaseous

79 species and X is the thickness of the skin-surface lipid layer [3]. While this is a reasonable

80 approximation when $k_{\text{p\_b}}$ is less than or comparable to v_{d}, it is an inaccurate approximation when

81 v_{d} is much smaller than $k_{\text{p\_b}}$. For the latter condition, the steady-state level of the compound in

82 the skin-surface lipids is substantially less than the value for equilibrium partitioning. In this

83 case, τ_s is more accurately estimated as follows:

84 $\qquad \tau_s \sim (v_{\text{d}}/k_{\text{p\_b}}) \times (K_{\text{lg}}\, X/v_{\text{d}}) = K_{\text{lg}}\, X/k_{\text{p\_b}}$ (S7)

85 This alternative expression reflects the fact that, when transport across the stratum corneum is

86 fast compared with the rate of external mass transfer (i.e., $k_{\text{p\_b}} \gg v_{\text{d}}$), the steady-state

87 concentration of the species at the air-skin interface, C_{gi}, is reduced:

88 $\qquad C_{\text{gi}} \sim (v_{\text{d}}/k_{\text{p\_b}}) \times C_{\text{g}}$ (S8)

89 As a consequence, the time scale to establish concentration profiles for steady flux is smaller

90 than estimated by equation (S6), which applies for conditions when $k_{\text{p\_b}} \gg v_{\text{d}}$.

91 $\qquad$ In our 2012 paper [3] we equated the equilibrium partitioning between the gas phase and the

92 skin-surface lipids, K_{lg}, with $K_{\text{sc\_g}}$. Upon further consideration, based in part on the analysis

93 presented by Nitsche et al. [4], we now consider this to be a poor assumption. Instead, we return

94 to the assumption that we used in our 2008 paper [5] that K_{lg} can be approximated as the

95 coefficient for equilibrium partitioning between octanol and air, K_{og}. That is, we assume that the

96   solubility of an organic in skin surface lipids is similar to that in octanol. The relationship

97   between K_{sc_g}, as calculated in the present paper, and K_{og} is displayed in Figure S3.

98   Table S2 lists estimates of τ_s for three cases: i) using equation (S7) when k_{p_b} is 17 m h^{-1} or

99   larger; ii) using equation (S6) when k_{p_b} is 0.79 m h^{-1} or smaller; and iii) using both equations

100   when k_{p_b} lies between 17 and 0.79 m h^{-1}. In making these calculations we have assumed that the

101   average lipid layer thickness is $X \sim 1$ µm [6] and that the external mass transfer coefficient to the

102   skin is $v_d \sim 6$ m h^{-1}. As a rough guide, τ_s is more than a day for organics with molecular weights

103   larger than 225 g/mol and log $(K_{og}) > 8$. A value of log (K_{og}) of 8 corresponds to log $(K_{sc\_g}) \sim 7$;

104   see Figure S3. Note that among the nineteen compounds with modeled D/I greater than 10,

105   approximately half (nine of 19) have estimated τ_s values longer than a day. However, even if

106   there is insufficient time to strictly justify the use of a steady-flux two-resistor model for

107   evaluating transport from air through the skin to blood, one would still conclude that these

108   compounds are absorbed by skin at a rate that is larger than inhalation intake into the body. For

109   $D/I > 1$, twenty-three of thirty-three compounds have τ_s values shorter than a day. The

110   corresponding proportions are seventeen of twenty for compounds with $0.1 < D/I < 1$ and 100%

111   for compounds with $D/I < 0.1$. Overall, the steady-state approximation is deemed reasonable for

112   a majority of the compounds considered, including half of the compounds for which the

113   maximum dermal uptake rate is much larger than the maximum inhalation intake rate.

114   **S4. Comparison with ten Berge model predictions.** Wil ten Berge has developed a

115   spreadsheet application (SkinPermMultiScen v1.1; http://home.wxs.nl/~wtberge/qsarperm.html)

116   for semi-empirical estimation of the permeation of substances (neat liquids, aqueous solutions

117   and vapors) through the skin; it is a refinement of an earlier dermal absorption model [7, 8]. This

118   model is also the basis for the American Industrial Hygiene Association's *IH SkinPerm* [9].

119   There are several differences in the derivation of ten Berge's semi-empirical model compared to

120   the model that we have presented. The ten Berge model calculates v_d for each compound rather

121   than using a fixed value for every compound. A quantitative structure–activity relationship

122   (QSAR) is used to estimate permeation through the transcellular and intercellular pathways in

123   the stratum corneum in contrast to using the Mitragotri model, as is done in the present paper.

124   Finally, ten Berge has used EPA's EpiSuite to estimate the parameters needed to calculate k_{p_g},

125   whereas we have used SPARC. For thirty-six compounds, Figure S6 compares values of k_{p_g}

126   calculated using the approach presented in the present paper with values calculated using the ten

127   Berge model. For compounds with k_{p_g} larger than 1.0 m/h in Table S1, the ten Berge model

128   predicts k_{p_g} values that are roughly 60% of those in Table S1. For compounds with k_{p_g} smaller

129   than 1 m/h, the ten Berge model predicts values that are typically larger than those in Table S1.

130   Overall, the strong qualitative and fair quantitative agreement between estimates made with these

131   two models is sufficient to reinforce the message that the transdermal pathway should be

132   considered when evaluating exposures to indoor organic pollutants.

133

134   **Nomenclature (for primary paper and for supporting information)**

135   Dimensions: L — length; M — mass; T — time

136   B — ratio of stratum corneum permeability to viable epidermis permeability (—)

137   BSA — body surface area (L^2)

138   C_g — gas-phase concentration of an organic compound ($M\,L^{-3}$)

139   C_{gi} —steady-state gas-phase concentration of the species at the air-skin interface ($M\,L^{-3}$)

140   C_p — particle-phase concentration of an airborne organic compound ($M\,L^{-3}$)

141   D — dermal uptake rate ($M\,T^{-1}$)

142   f_g — fraction of the airborne organic that is in the gas phase (—)

143   f_{om} — fraction of airborne particulate matter that is organic (—)

144   H — Henry's law constant, with units of (mole/liter) per atmosphere

145   I — inhalation intake rate (M T^{-1})

146   J — transdermal flux of an organic compound (M L^{-2} T^{-1})

147   k_{p_b} — permeability coefficient for transport of a gas-phase organic compound from the gaseous

148   boundary layer at the skin surface (b) through the stratum corneum/viable epidermis

149   composite to dermal capillaries (L T^{-1})

150   k_{p_cw} — permeability coefficient through the stratum corneum (c) of an organic compound when

151   the species concentration is measured in water (w) in contact with skin (L T^{-1})

152   k_{p_ew} — permeability coefficient through the viable epidermis (L T^{-1})

153   k_{p_g} — indoor air transdermal permeability coefficient for transport of a gas-phase organic from

154   the bulk air of a room through the boundary layer adjacent to skin and then through the

155   stratum corneum/viable epidermis composite to dermal capillaries (L T^{-1})

156   k_{p_w} — permeability coefficient for an organic from water in contact with the skin through the

157   stratum corneum and viable epidermis composite (L T^{-1})

158   K_{lg} — coefficient of equilibrium partitioning for an organic compound between skin-surface

159   lipids and the gas phase (—)

160   K_{og} — coefficient of equilibrium partitioning for an organic compound between octanol and air

161   (—)

162   K_{ow} — coefficient of equilibrium partitioning for an organic compound between octanol and

163   water (—)

164   K_p — coefficient of equilibrium partitioning of an organic compound between the gas phase and

165   airborne particulate matter (—)

166   K_{sc_g} — coefficient of equilibrium partitioning for an organic compound between the stratum

167   corneum and the gas phase (—)

168   MW — molecular weight of compound (g mol^{-1})

169   P_s — organic compound's vapor pressure (atm)

170   Q_b — volumetric breathing rate; estimated as 0.5 m^3 h^{-1} for an adult at rest (L^3 T^{-1})

171   R — the gas constant (0.082 atmosphere liter/(K mole))

172   T — temperature (K or °C)

173   TSP — total suspended particulate matter mass concentration (M L^{-3})

174   v_d — mass-transfer coefficient for external transport of an organic compound from the gas phase

175   in the core of a room through the boundary layer adjacent to the skin (L T^{-1})

176   X — thickness of the skin-surface lipids (L)

177   ρ_{part} — density of airborne particulate matter (M L^{-3})

178   τ_s — time scale needed for a species in skin-surface lipids to equilibrate with its gaseous

179   concentration by means of gas-phase mass transfer (T)

180

References

182   1. Mitragotri, S. A theoretical analysis of permeation of small hydrophobic solutes across the

183   stratum corneum based on scaled particle theory. *J. Pharm. Sci.* **2002**, *91*, 744-752.

184   2. Bunge, A. L.; Cleek, R. L.; Vecchia, B. E. A new method for estimating dermal absorption

185   from chemical exposure. 3. Compared with steady-state methods for prediction and data

186   analysis. *Pharm. Res.* **1995**, *12*, 972-982.

187   3. Weschler, C. J.; Nazaroff, W. W. SVOC exposure indoors: fresh look at dermal pathways.

188   *Indoor Air* **2012**, *22*, 356-377.

189   4. Nitsche, J. M.; Wang, T.-F.; Kasting, G. B. A two-phase analysis of solute partitioning into

190   the stratum corneum. *J. Pharm. Sci.* **2006**, *95*, 649-666.

191   5. Weschler, C. J.; Nazaroff, W. W. Semivolatile organic compounds in indoor environments. *Atmos. Environ.* **2008**, *42*, 9018-9040.

193   6. Nicolaides, N. Skin lipids: their biochemical uniqueness. *Science* **1974**, *186*, 19-26.

194   7. Wilschut, A.; ten Berge, W. F.; Robinson, P. J.; McKone, T. E. Estimating skin permeation. The validation of five mathematical skin permeation models. *Chemosphere* **1995**, *30*, 1275-1296.

197   8. ten Berge, W. A simple dermal absorption model: Derivation and application. *Chemosphere* **2009**, *75*, 1440-1445.

199   9. Tibaldi , R.; ten Berge, W.; Drolet, D. Dermal absorption of chemicals: estimation by IH SkinPerm, *J. Occup. Environ. Hyg.* **2014**, *11*, 19-31.

201   10. Wang, T. F.; Kasting, G. B.; Nitsche, J. M. A multiphase microscopic diffusion model for stratum corneum permeability. II. Estimation of physicochemical parameters, and application to a large permeability database. *J. Pharm. Sci.* **2007**, *96*, 3024-3051.

206 **Table S1.** For selected organics that are found indoors and exist primarily in the gas phase,
207 relevant physical and chemical properties (MW, K_{ow}, H, K_{sc_g}) ratio of stratum corneum to viable
208 epidermis permeability (B), permeability coefficient (k_{p_g}), modeled steady-state ratio of dermal
209 uptake to inhalation intake (D/I) of gas-phase species and fraction of organic in the gas-phase
210 (f_g); compounds rank ordered according to D/I.

Compound	MW g/mol	log (K_{ow}) [—][a]	log (H)[a] (mol/liter) atm^{-1}	log (K_{sc_g}) [—][a]	B[a] [—]	k_{p_g} m/h	D/I [—]	f_g [—]
diethanolamine	105	-2.5	8.68	8.2	<0.001	6.0	24	1.00
2,4-D[b]	221	2.9	5.16	8.7	0.026	5.8	23	0.98
butyl paraben	194	3.4	4.10	8.0	0.097	5.4	22	0.99
propyl paraben	180	2.8	4.22	7.7	0.048	5.2	21	1.00
ethyl paraben	166	2.2	4.39	7.4	0.023	4.9	20	1.00
di(n-butyl) phthalate	278	4.6	3.61	8.4	0.17	4.8	19	0.97
methyl paraben	152	1.5	4.61	7.1	0.010	4.7	19	1.00
o-phenylphenol	170	3.5	3.42	7.4	0.18	4.6	18	1.00
di(isobutyl) phthalate	278	4.2	3.76	8.3	0.092	4.6	18	0.98
nicotine[b]	162	2.0	4.31	7.2	0.017	4.4	18	1.00
diethyl phthalate	222	2.6	4.06	7.3	0.016	3.4	14	1.00
diazinon	304	4.9	3.10	8.1	0.18	3.3	13	0.98
dimethyl phthalate	194	1.5	4.45	6.9	0.0043	2.9	12	1.00
Galaxolide (HHCB)	258	4.6	2.85	7.6	0.22	2.8	11	0.99
Tonalide (AHTN)	258	5.0	2.58	7.7	0.44	2.6	11	0.99
monoethanolamine	61	-1.8	5.32	5.4	<0.001	2.5	9.9	1.00
nonylphenol	220	6.2	2.00	8.0	5.9	2.3	9.3	0.97
Phantolide	244	4.8	2.35	7.3	0.40	1.8	7.4	1.00
pentachlorophenol[b]	266	4.9	2.30	7.3	0.36	1.6	6.2	1.00
Texanol	216	2.4	3.46	6.7	0.014	1.4	5.5	1.00
ethylene glycol	62	-1.4	4.62	5.0	<0.001	1.2	5.0	1.00
hexyl cinnamal	216	5.0	1.86	6.9	0.88	1.2	4.8	1.00
n-methyl pyrrolidone	99	0.063	3.97	5.4	0.002	1.2	4.8	1.00
α-terpineol	154	2.5	2.72	6.0	0.045	0.98	3.9	1.00
phenol	94	1.5	2.62	5.2	0.029	0.70	2.8	1.00
eugenol	164	3.2	2.12	5.9	0.12	0.6	2.5	1.00
4-oxopentanal	100	0.10	3.57	5.0	0.003	0.56	2.2	1.00
chlorpyrifos	351	6.4	1.39	7.5	1.0	0.41	1.6	0.99
linalool	154	3.2	1.85	5.6	0.13	0.40	1.6	1.00
BHT	220	4.7	1.44	6.3	0.50	0.38	1.5	1.00
2-butoxyethanol	118	1.1	2.78	5.0	0.010	0.33	1.3	1.00
dimethylacetamide	87	-0.18	3.37	4.6	0.002	0.32	1.3	1.00
p-tert-bucinal	204	4.0	1.52	5.9	0.22	0.26	1.0	1.00
aniline	93	0.99	2.43	4.6	0.012	0.21	0.84	1.00
2-ethoxyethanol	90	0.058	3.07	4.4	0.002	0.19	0.74	1.00
methyl ionone	206	4.1	1.31	5.8	0.26	0.18	0.74	1.00
1-octen-3-ol	128	2.79	1.49	5.0	0.11	0.18	0.71	1.00
PCB28	258	5.5	0.84	6.3	1.1	0.14	0.58	1.00

2-methoxyethanol	76	-0.66	3.21	4.1	0.001	0.14	0.56	1.00
furfural	96	0.38	2.70	4.4	0.004	0.14	0.56	1.00
1-methoxy-2-propanol	90	-0.35	3.13	4.3	0.001	0.13	0.54	1.00
PCB52	292	6.1	0.74	6.7	1.7	0.13	0.52	1.00
α-chlordane	410	6.5	1.02	7.2	0.53	0.11	0.46	0.99
γ-chlordane	410	6.5	1.02	7.2	0.53	0.11	0.46	1.00
geranyl acetone	208	5.3	0.58	5.9	1.6	0.10	0.41	1.00
hexanol	102	2.1	1.44	4.4	0.060	0.10	0.40	1.00
3-octanol	130	2.80	1.16	4.6	0.11	0.083	0.33	1.00
dimethylformamide	73	-0.55	2.86	3.9	0.002	0.081	0.33	1.00
benzyl acetate	150	2.2	1.59	4.6	0.030	0.060	0.24	1.00
butanol	74	1.0	1.64	3.7	0.016	0.053	0.21	1.00
cyclohexanone	98	1.0	1.81	4.0	0.011	0.048	0.19	1.00
isobutanol	74	0.76	1.68	3.6	0.012	0.043	0.17	1.00
nitrobenzene	123	1.8	1.35	4.1	0.026	0.033	0.13	1.00
methyl glyoxal	72	-0.70	2.42	3.3	0.001	0.024	0.096	1.00
naphthalene	128	3.3	0.17	4.0	0.25	0.017	0.067	1.00
glyoxal	58	-1.1	2.32	2.9	0.001	0.015	0.060	1.00
nonanal	142	3.6	-0.03	4.0	0.31	0.012	0.049	1.00
3-octanone	128	2.86	0.18	3.7	0.13	0.0099	0.040	1.00
hexanal	100	2.0	0.42	3.3	0.050	0.0081	0.033	1.00
methyl ethyl ketone	72	0.75	0.90	2.9	0.012	0.0075	0.030	1.00
tetrahydrofuran	72	0.44	0.99	2.7	0.008	0.0056	0.022	1.00
acrolein	56	0.37	0.73	2.4	0.009	0.0043	0.017	1.00
p-dichlorobenzene	147	3.1	-0.34	3.3	0.12	0.0027	0.011	1.00
styrene	104	2.9	-0.63	2.9	0.20	0.0025	0.010	1.00
o-xylene	106	2.9	-0.84	2.7	0.22	0.0016	0.0065	1.00
m-xylene	106	3.0	-0.95	2.7	0.24	0.0014	0.0056	1.00
p-xylene	106	3.0	-0.90	2.7	0.25	0.0016	0.0063	1.00
toluene	92	2.5	-0.96	2.3	0.15	0.0010	0.0038	1.00
formaldehyde	30	-0.55	0.32	1.3	0.004	0.00087	0.0035	1.00
benzene	78	2.0	-0.92	1.9	0.080	0.00066	0.0026	1.00
limonene	136	4.6	-1.93	2.8	1.7	0.00041	0.0017	1.00
chloroform	119	1.6	-0.58	2.0	0.018	0.00028	0.0011	1.00
isoprene	68	2.4	-1.81	1.3	0.18	0.00019	0.00076	1.00
1,1,1-trichloroethane	133	2.5	-1.31	1.9	0.062	0.00016	0.00065	1.00
α-pinene	136	4.5	-2.51	2.2	1.6	0.00011	0.00043	1.00
trichloroethylene	131	2.7	-1.74	1.7	0.10	0.00009	0.00036	1.00
tetrachloroethylene	166	3.4	-1.93	2.0	0.16	0.00008	0.00032	1.00
hexane	86	3.7	-3.11	1.1	1.1	0.00003	0.00012	1.00
undecane	156	6.5	-3.84	2.4	29	0.00001	0.00003	1.00

211 [a] Computed for $T = 32\ °C$. [b] Compound assumed nonionized. Abbreviations: 2,4-D – 2,4-
212 dichlorophenoxyacetic acid; BHT – butylated hydroxy toluene; PCB28 – 2,4,4′-trichlorobiphenyl; PCB52
213 – 2,2′,5,5′-tetrachlorobiphenyl.
214

215 **Table S2.** For the organics listed in Table S1, molecular weights (MW), parameters used to
216 estimate τ_s (K_{og}, k_{p_b}) and values of τ_s estimated using equation (S6) ($K_{og} X/v_d$) or equation (S7)
217 ($K_{og} X/k_{p\_b}$) with compounds rank ordered as in Table S1.

Compound	MW g/mol	log (K_{og}) [—]	k_{p_b} m/h	τ_s estimated as ($K_{og} X/v_d$)[a] h	τ_s estimated as ($K_{og} X/k_{p\_b}$)[b] h
diethanolamine	105	7.6	1030		0.04
2,4-D[b]	221	9.4	162		16
butyl paraben	194	8.9	52		15
propyl paraben	180	8.4	37		7
ethyl paraben	166	8.0	28		4
di(n-butyl) phthalate	278	9.6	23		160
methyl paraben	152	7.6	21		2
o-phenylphenol	170	8.3	20		11
di(isobutyl) phthalate	278	9.3	19		120
nicotine[b]	162	7.7	17		3
diethyl phthalate	222	8.0	7.9	17	13
diazinon	304	9.4	7.3	400	310
dimethyl phthalate	194	7.3	5.7	3	4
Galaxolide (HHCB)	258	8.8	5.3	110	120
Tonalide (AHTN)	258	9.0	4.7	150	190
monoethanolamine	61	4.9	4.2	0.01	0.02
nonylphenol	220	9.6	3.8	700	1100
Phantolide	244	8.5	2.7	60	120
pentachlorophenol[b]	266	8.6	2.1	70	190
Texanol	216	7.3	1.8	3	11
ethylene glycol	62	4.6	1.6	0.01	0.03
hexyl cinnamal	216	8.2	1.5	30	120
n-methyl pyrrolidone	99	5.4	1.5	0.05	0.18
α-terpineol	154	6.6	1.2	0.7	4
phenol	94	5.6	0.79	0.06	
eugenol	164	6.7	0.7	0.9	
4-oxopentanal	100	5.1	0.61	0.02	
chlorpyrifos	351	9.1	0.43	200	
linalool	154	6.4	0.43	0.4	
BHT	220	7.5	0.40	5	
2-butoxyethanol	118	5.3	0.35	0.03	
dimethylacetamide	87	4.6	0.34	0.01	
p-tert-bucinal	204	6.9	0.27	1.4	
aniline	93	4.8	0.22	0.01	
2-ethoxyethanol	90	4.4	0.19	< 0.01	
methyl ionone	206	6.8	0.20	1.1	
1-octen-3-ol	128	5.7	0.18	0.08	
PCB28	258	7.8	0.15	10	
2-methoxyethanol	76	4.0	0.14	< 0.01	
furfural	96	4.5	0.14	0.01	

12

1-methoxy-2-propanol	90	4.2	0.14	< 0.01	
PCB52	292	8.3	0.13	30	
α-chlordane	410	8.9	0.12	120	
γ-chlordane	410	8.9	0.12	120	
geranyl acetone	208	7.3	0.11	3	
hexanol	102	4.9	0.10	0.01	
3-octanol	130	5.4	0.084	0.04	
dimethylformamide	73	3.7	0.082	< 0.01	
benzyl acetate	150	5.2	0.061	0.03	
butanol	74	4.0	0.053	< 0.01	
cyclohexanone	98	4.2	0.048	< 0.01	
isobutanol	74	3.8	0.043	<0.01	
nitrobenzene	123	4.6	0.033	0.01	
methyl glyoxal	72	3.1	0.024	< 0.01	
naphthalene	128	4.8	0.017	0.01	
glyoxal	58	2.6	0.015	< 0.01	
nonanal	142	4.9	0.012	0.01	
3-octanone	128	4.4	0.010	<0.01	
hexanal	100	3.8	0.0081	< 0.01	
methyl ethyl ketone	72	3.1	0.0075	< 0.01	
tetrahydrofuran	72	2.8	0.0056	< 0.01	
acrolein	56	2.5	0.0043	< 0.01	
p-dichlorobenzene	147	4.1	0.0027	< 0.01	
styrene	104	3.6	0.0025	< 0.01	
o-xylene	106	3.5	0.0016	< 0.01	
m-xylene	106	3.5	0.0014	< 0.01	
p-xylene	106	3.5	0.0016	< 0.01	
toluene	92	3.0	0.0010	< 0.01	
formaldehyde	30	1.2	0.00087	< 0.01	
benzene	78	2.5	0.00066	< 0.01	
limonene	136	4.0	0.00041	< 0.01	
chloroform	119	2.4	0.00028	< 0.01	
isoprene	68	2.0	0.00019	< 0.01	
1,1,1-trichloroethane	133	2.6	0.00016	< 0.01	
α-pinene	136	3.4	0.00011	< 0.01	
trichloroethylene	131	2.4	0.00009	< 0.01	
tetrachloroethylene	166	2.9	0.00008	< 0.01	
hexane	86	2.0	0.00003	< 0.01	
undecane	156	4.1	0.00001	< 0.01	

218   [a] K_{og} used to approximate K_{lg} (see text); $X \sim 1$ μm; $v_d \sim 6$ m h^{-1}.   [b] K_{og} used to approximate K_{lg} (see text);
219    $X \sim 1$ μm.
220

221   **Table S3.** For a subset of compounds from Table S1, a comparison of k_{p_g} values calculated
222   using the procedure in the *Methods* section of this paper for fully hydrated stratum corneum with
223   values calculated using the procedure outlined in Wang et al. [10] for partially hydrated stratum
224   corneum.

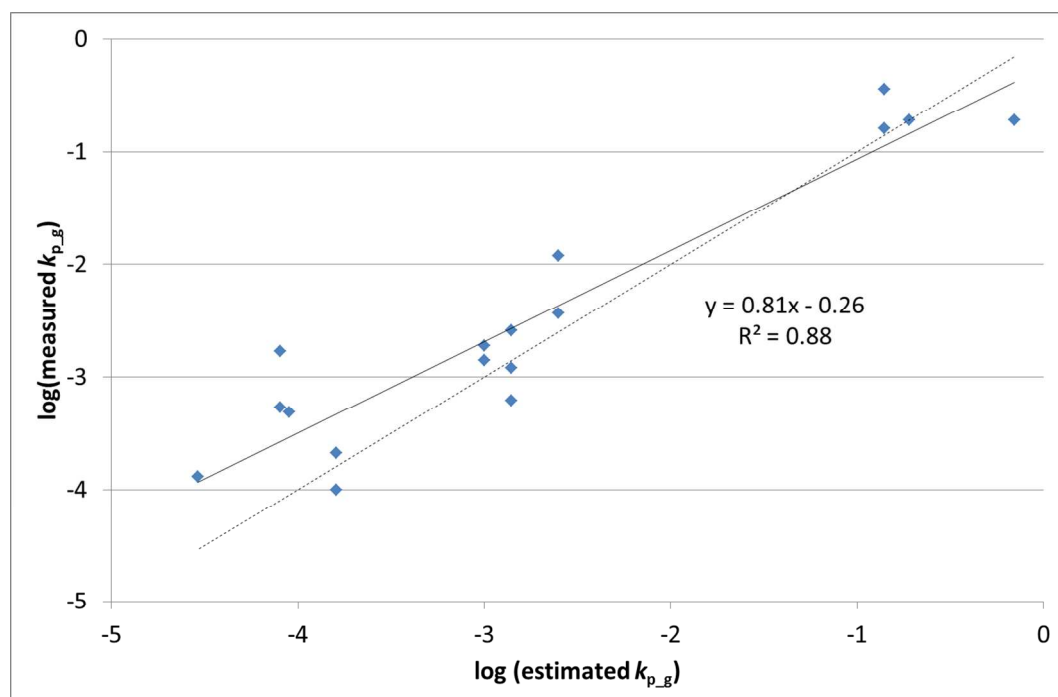| Compound	k_{p_g} [fully hydrated stratum corneum] m/h	k_{p_g} [partially hydrated stratum corneum] m/h
butyl paraben	5.4	4.7
propyl paraben	5.2	4.1
ethyl paraben	4.9	3.5
di(n-butyl) phthalate	4.8	4.4
methyl paraben	4.7	2.8
di(isobutyl) phthalate	4.6	3.9
diethyl phthalate	3.4	1.8
dimethyl phthalate	2.9	1.1
Galaxolide (HHCB)	2.8	2.3
Tonalide (AHTN)	2.6	2.4
Phantolide	1.8	1.6
Texanol	1.4	0.53
α-terpineol	0.98	0.36
phenol	0.70	0.22
eugenol	0.63	0.28
4-oxopentanal	0.56	0.12
linalool	0.40	0.17
m-xylene	0.0014	0.00065

225

226

Figure S1. Measured versus modeled values for k_{p_g} ($n = 17$; MW = 76-166 g/mol). Dashed line: slope = 1.00, intercept = 0. Solid line: least-squares regression with fit reported in the figure.
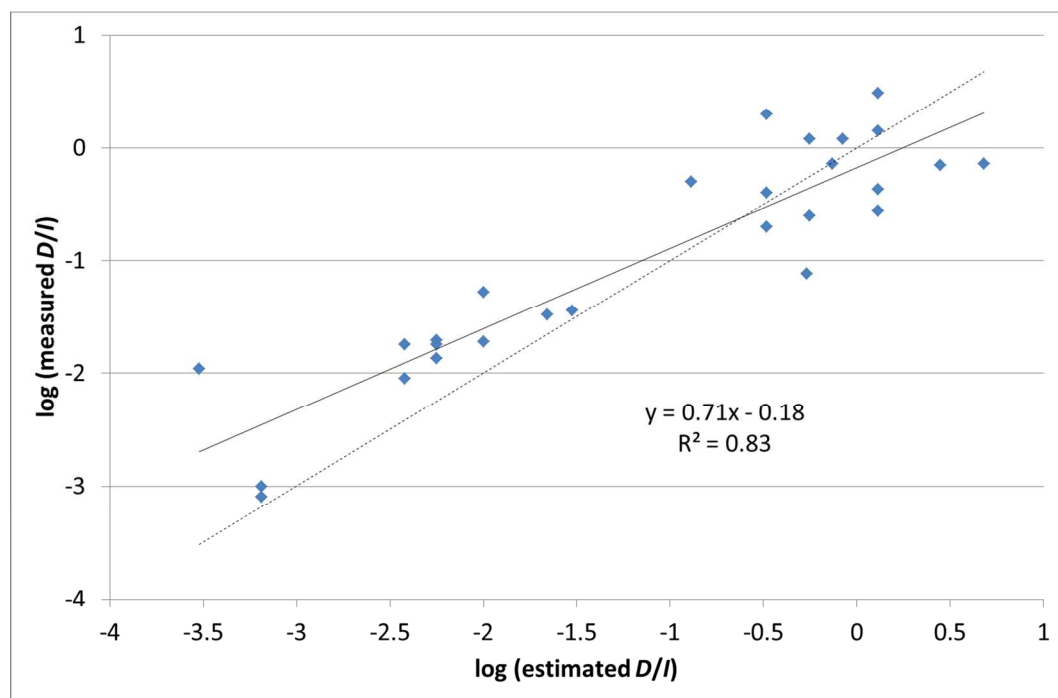
230
231

232

Figure S2. Measured versus modeled values for D/I ($n = 27$; MW = 72-166 g/mol). Dashed line: slope = 1.00, intercept = 0. Solid line: least-squares regression with fit reported in the figure.
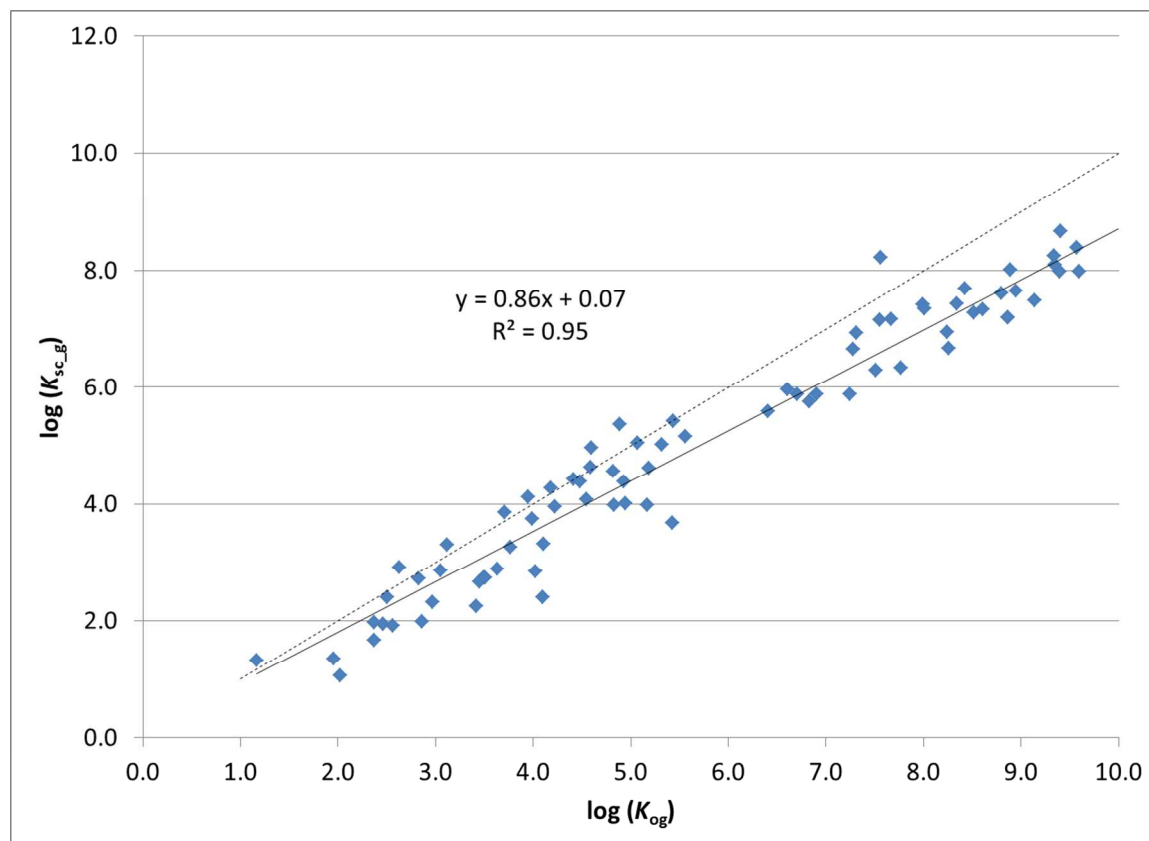
235

15

$$y = 0.86x + 0.07$$
$$R^2 = 0.95$$

236
237
238 **Figure S3.** For the compounds listed in Table S1, the relationship between log (K_{sc_g}) and log
239 (K_{og}). Values calculated using SPARC v4.6. Dashed line: slope = 1.00, intercept = 0.0. Solid
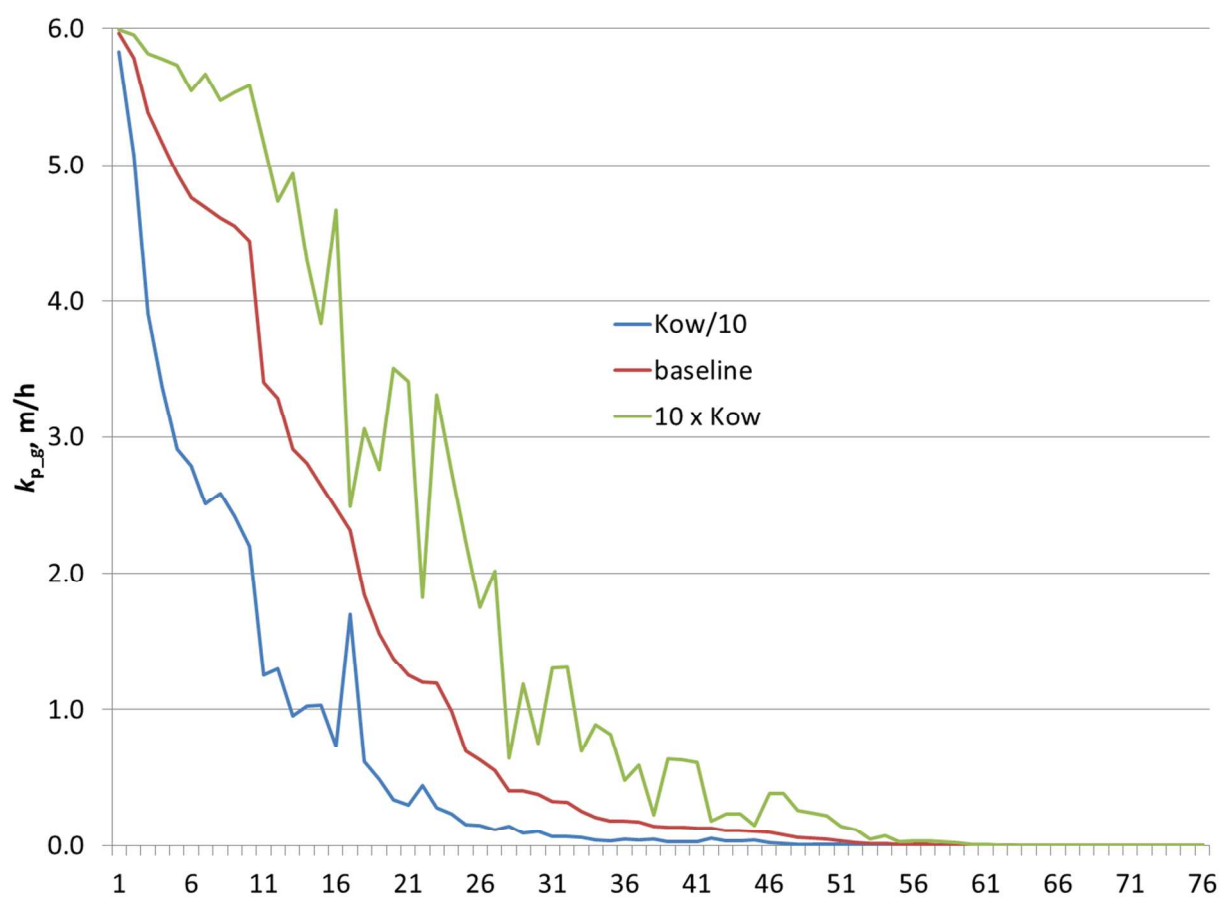240 line: least-squares regression with fit reported in the figure.
241

242

243
244

Figure S4. Sensitivity of k_{p_g} to an order of magnitude change in K_{ow}. Numbers on the *x*-axis correspond to the order in which compounds are listed in Table S1: 1 – diethanolamine; 2 – 2,4-D; 3 – butyl paraben, etc.
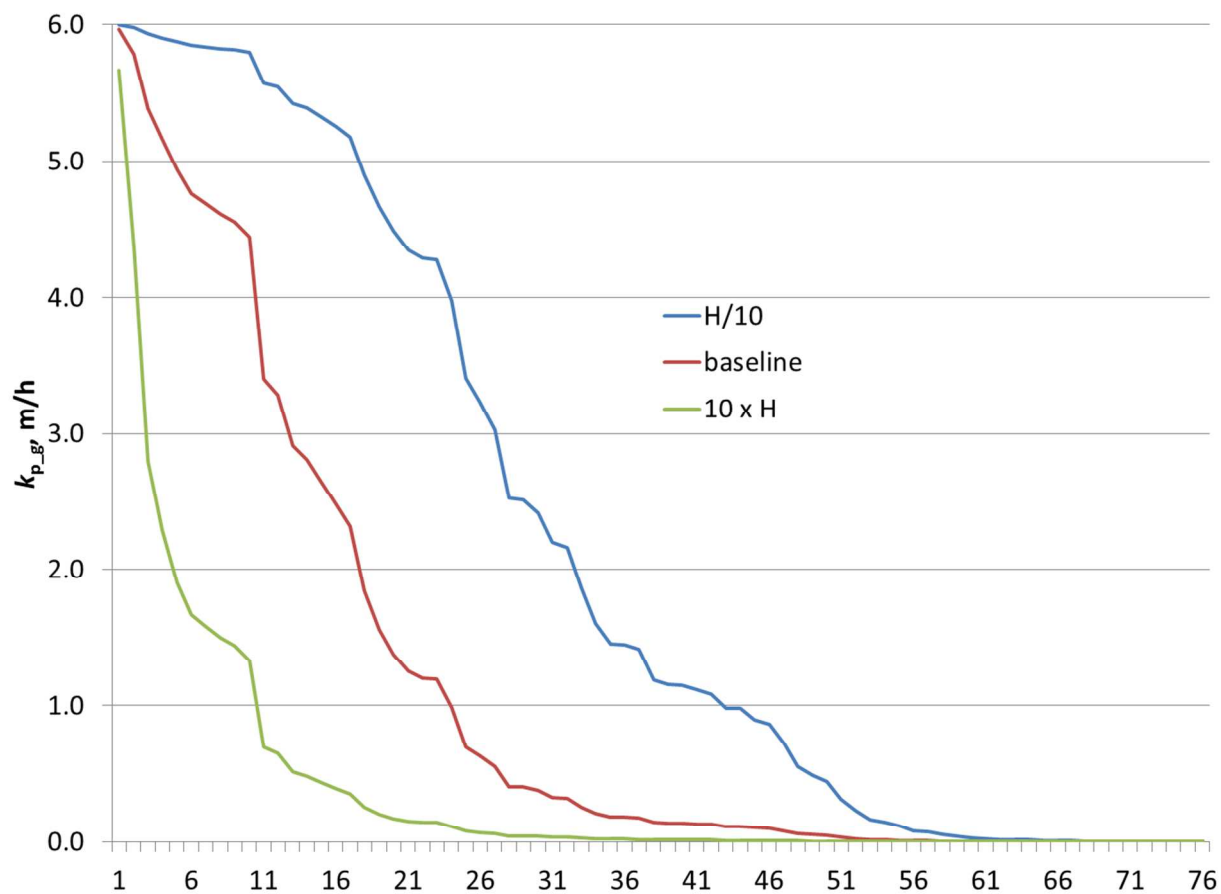
248
249
250

Figure S5. Sensitivity of k_{p_g} to an order of magnitude change in H. Numbers on the x-axis correspond to the order in which compounds are listed in Table S1: 1 – diethanolamine; 2 – 2,4-D; 3 – butyl paraben, etc.
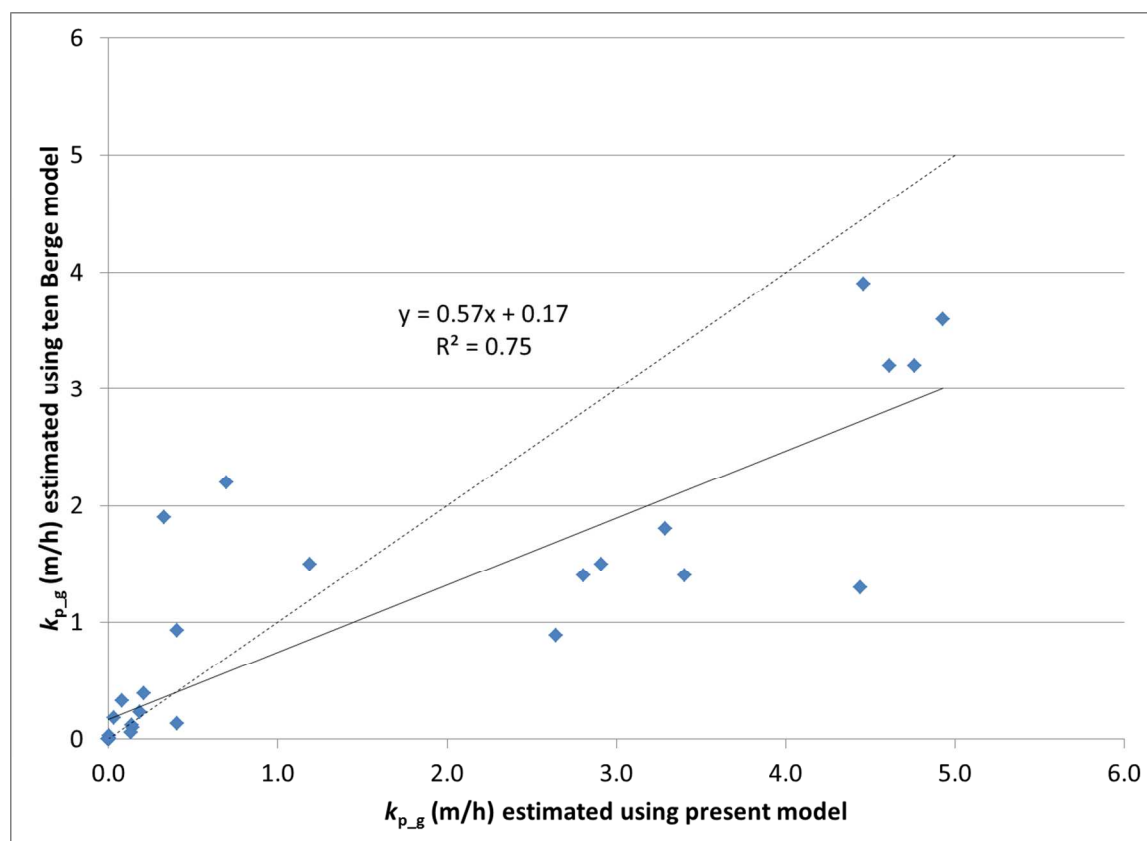
The figure shows a scatter plot with axis labels "k_{p_g} (m/h) estimated using ten Berge model" on the y-axis (ranging 0 to 6) and "k_{p_g} (m/h) estimated using present model" on the x-axis (ranging 0.0 to 6.0). The fit equation is:

y = 0.57x + 0.17
R^2 = 0.75

257
258
259 **Figure S6.** Comparisons between k_{p_g} estimated using the approach presented in the present
260 paper and that presented by ten Berge (SkinPermMultiScen v1.1). Dashed line: slope = 1.00,
261 intercept = 0.0. Solid line: least-squares regression with fit reported in the figure.
262